GEOPHYSICS, VOL. 54, NO. 4 (APRIL 1989); P. 514–523, 15 FIGS.

Induced-polarization effects in time-domain electromagnetic measurements

Marcus F. Flis*, Gregory A. Newman‡, and Gerald W. Hohmann§

ABSTRACT

Sign reversals in the coincident-loop transient response can be produced by employing a Cole-Cole model in numerical TEM modeling of polarizable conductors. These reversals may be thought of in terms of a polarization current which changes sign during the transient, passing from a charging current at early times to a discharging current at late times. In a layered earth, the relative strength of this current compared to the normally induced vortex current dictates whether or not a reversal is seen. If the earth is conductive, the effects of the polarization current may never be seen. If, however, the earth is only moderately conductive, the polarization current may dominate.

In the case of a 3-D polarizable conductor in a conductive host, the addition of a host response serves to delay the time of any sign reversal in the transient. Reducing the host rock response by increasing its resistivity enables the polarization current to dominate earlier. By bringing the conductor closer to the surface, the amplitude of the negative response can be made greater and hence the sign reversal brought earlier in time. In such cases, moderate polarization parameters may cause substantial negative responses.

It is possible to interpret TEM anomalies exhibiting sign reversals. The location and geometry of a discrete polarizable conductor can be correctly assessed, and a valid but approximate TEM time constant can be measured, from the positive part of the transient before the sign reversal.

INTRODUCTION

While the transient electromagnetic (TEM) method is widely used in many areas of geologic investigations, the ability to model quantitatively realistic earth structures has only recently become available. Scale and numerical modeling techniques, such as those of Dyck et al. (1980), Knight and Raiche (1982), Ogilvy (1983), and San Filipo and Hohmann (1985), have allowed a greater understanding of the physical processes involved.

The appearance of negative transients in coincident-loop data (Spies, 1980a), which could not be explained using nondispersive resistivities (Weidelt, 1982), has prompted investigations into the effects of polarizable media on TEM measurements. Morrison et al. (1969) established that these effects, termed induced-polarization (IP) effects, may manifest themselves as sign reversals in coincident-loop transients. Hohmann et al. (1970) carried out both theoretical and practical studies into detecting sign reversals with a frequency-domain EM system. Their results indicated that IP effects were not detectable with such systems using amplitude data only.

Subsequent workers investigated the detectability of IP effects using numerical modeling of the TEM method. A polarizable sphere in free space was studied by Lee (1975), while Weidelt (1982) presented an example of IP effects caused by a polarizable conducting loop. Polarizable whole and half-spaces were studied by Lee (1981), Wait and Debroux (1984), and Raiche (1983). Lewis and Lee (1984) calculated the response of a polarizable 2-D horizontal cylinder in a half-space.

The aim of this paper is to examine the behavior of a polarizable earth, first by investigating the layered earth and then by extending the study to the important class of 3-D conductors in a conductive half-space. The insight gained from this study is then applied to field TEM data displaying IP effects.

INDUCED POLARIZATION AND THE COLE-COLE IMPEDANCE MODEL

Our impedance model for a polarizable earth is described by the empirical Cole-Cole model (Pelton, 1977)

$$Z(\omega) = R_0\left\{1 - M\left(1 - 1/[1 + (i\omega\tau)^c]\right)\right\},$$

Manuscript received by the Editor July 31, 1987; revised manuscript received October 6, 1988.
*CRA Exploration Pty. Ltd., P.O. Box 683, Broken Hill, N.S.W. 2880, Australia.
‡Institut fur Geophysik und Meteorologie, Universitat zu Koln Albertus Magnus Platz, 5000 Koln 41, West Germany.
§Department of Geology and Geophysics, University of Utah, Salt Lake City, UT 84112

where $Z(\omega)$ is the impedance at frequency ω, R_0 is the dc resistivity, M is the chargeability, τ is the IP time constant, and c is the exponent describing the variation of phase with frequency. This model is selected because its parameters may be related to physical rock properties and it can be used to generate many of the other popular impedance models (Pelton, 1977). The question of what ranges the Cole-Cole parameters can assume is not within the scope of this paper. As a guide, studies by Pelton (1977) and Lewis and Bishop (1988) indicate that values of $M = 0$ to 0.98, $\tau = 1 \times 10^{-3}$ to 5×10^{3} s, and $c = 0.1$ to 0.6 are not unreasonable. R_0 is typically in the range 1×10^{-4} to 1×10^{5} $\Omega \cdot$m. In this paper, strong polarizabilities are used, allowing IP effects to be readily observed.

Of particular interest is the behavior of the Cole-Cole model over a broad frequency range. Figure 1 shows the phase spectra of a Cole-Cole impedance for $\tau = 0.001$ s, $c = 0.25$, and $M = 0.1$, 0.2, 0.3, and 0.4. While in the conventional IP frequency range only a few milliradians of phase change occur, the spectra actually peak at frequencies well above this range but notionally within that of TEM systems. At high frequencies, the Cole-Cole impedance asymptotically approaches $R_0(1 - M)$, while at low frequencies it asymptotically approaches R_0. Thus, through the Fourier transform, the effective resistivity decreases at early delay times in the time domain. This high-frequency decrease may be thought of as the reduction in resistivity prior to polarization resistance and the overvoltage reaction reaching a maximum in an electrically energized rock (Sumner, 1976).

The Cole-Cole model in TEM modeling is most easily implemented in the frequency domain, avoiding a convolution between the complex resistivity and the electric field.

LAYERED-EARTH MODELS

To gain insight into IP effects, the 1-D earth is studied first. The program used to compute responses for a layered earth is based on transforming frequency-domain results to the time domain employing the Gaver-Stehfest inverse Laplace transform (Knight and Raiche, 1982). Results were checked against an independent frequency-domain program using an inverse Laplace transform prior to a Hankel transform.

A coincident-loop configuration is chosen because sign reversals can be identified as IP and not geometric effects. The in-loop configuration, with a dipole receiver at the center of the transmitter loop, has essentially the same response but with a higher amplitude and occurring earlier in time (Spies, 1980b). The excitation current used in the modeling was a 1 A step function turnoff with no ramp. The calculated response was the emf, which is proportional to the time rate of change of the vertical component of the secondary magnetic field, integrated over the loop area.

A typical response for a polarizable half-space is compared with that for a nonpolarizable half-space in Figure 2. The emf for the polarizable case decays as approximately $t^{-2.5}$ at early delay times, changes sign at around 2 ms (for this particular model), and subsequently decays to zero. The classic IP mechanisms are invoked to explain this behavior, with the usual directly injected current being replaced by an induced vortex current. At the instant of transmitter current turnoff, vortex currents are induced in the earth beneath the transmitter loop.

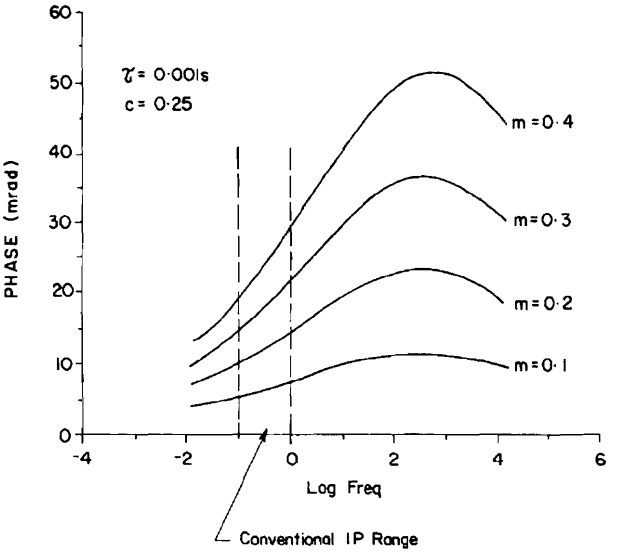

FIG. 1. Phase spectra for the Cole-Cole model: $M = 0.1$, 0.2, 0.3, and 0.4 with $\tau = 0.001$ s, $c = 0.25$. The abscissa units are powers of 10 in hertz.

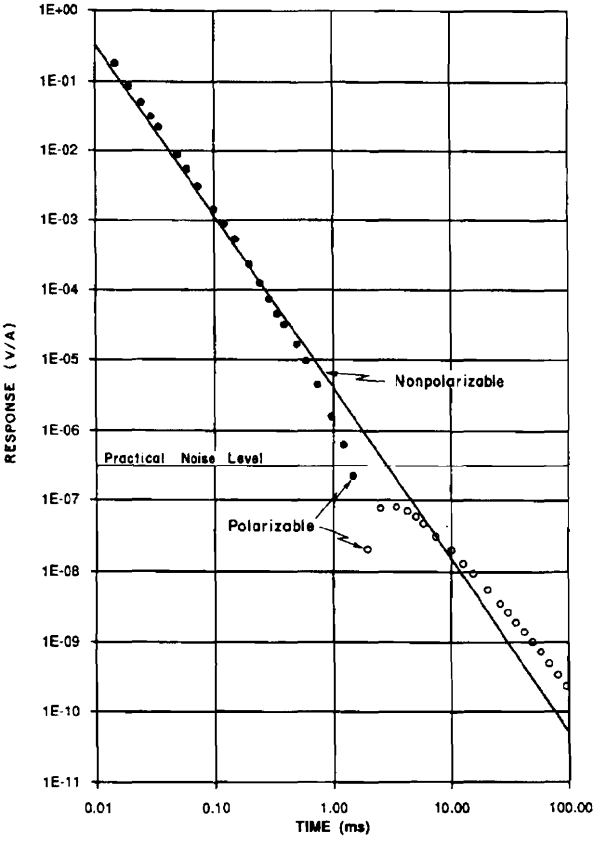

FIG. 2. Coincident-loop (100 m) transients for a half-space of 500 $\Omega \cdot$m. The transient due to a nonpolarizable earth is shown by a solid line, while circles denote that due to a polarizable earth with $M = 0.1$, $\tau = 0.001$s, and $c = 0.15$. Dots and lines represent positive values; open circles represent negative values. The noise level for practical TEM systems is indicated.

The sense of these currents is such as to support the rapidly decaying magnetic field. Ions in fluid-filled pore spaces within the rock are driven by this vortex current, conceptually creating an additional current flowing in the same direction as the vortex current. This additional current is termed the polarization current and can be thought of as being caused by the additional charge carriers supplied by the pore-space electrolyte. Once this initial ionic movement has ended by ions "piling up" at boundaries between regions of varying ion mobility, the "charged" state of a polarizable conductor is achieved. When the vortex current decays sufficiently, the ions return to the equilibrium position that existed prior to the induction of the vortex current. This ion flow again constitutes a polarization current, now in the opposite direction to that of the decaying vortex current but with a slower decay. If the earth is sufficiently polarizable, the polarization current may be large enough to dominate the vortex current, causing the emf to decay faster than normal and possibly reverse completely. This concept is illustrated in Figure 3, which shows a small volume of polarizable rock under the influence of a vortex current. Although polarization and vortex currents are coupled, their separation is justified on the grounds that the energy source for the vortex current is a collapsing magnetic field, while for the polarization current, the source is the capacitive nature of the IP phenomenon (membrane and electrode polarization). Also, inductive processes do not require the presence of ions in an electrolyte, while polarization processes do. Sidorov and Yakhin (1979) suggested a similar separation.

Since we are dealing with an impulsive source, it is instructive to map the total current which actually exists in the earth for the polarizable and nonpolarizable cases. The y component of the electric field, which is related to the current density if multiplied by the conductivity of the half-space, is mapped below the transmitter loop. This current density determines the magnetic field observed at the surface of the earth. Contours of the percentage difference between the electric fields due to both the polarizable earth of Figure 2 and the equivalent nonpolarizable earth are shown in Figure 4. At 0.1 ms, this difference is positive, indicating an enhanced current is present in the polarizable earth. By 10 ms, the difference is negative, the total current being depressed by the presence of the now negative polarization current. The early-time enhancement is a consequence of the polarizable earth being charged by the vortex current, a phenomenon not usually measured in conventional IP surveys. Since the IP phenomenon is linear, charge and decay curves being equal but opposite in sign (Sumner, 1976), TEM measurements taken immediately following transmitter turnoff will detect the positive polarization current.

The Cole-Cole parameters determine the amplitude of the polarization current and, therefore, dictate when the emf reverses. The time of the reversal, plotted as a function of the Cole-Cole parameters, is shown in Figure 5. For each curve, one parameter is varied while the others are held fixed. The IP time constant significantly affects the time of the sign reversal only at extreme values. Also, applying the work of Pelton (1977) on rock specimens as a guide, most rocks have a frequency dependence of around 0.25. In general then, the amplitude of the polarization current is expected to depend most strongly on the chargeability and dc resistivity of the medium: increasing R_0 decreases the strength of the vortex current, allowing the polarization current to dominate earlier, while increasing M increases the amplitude of the polarization current. While Figure 5 is specific to the particular 1-D model we studied, the general forms of the curves remain the same for other 1-D models.

Interpretation of layered-earth responses

Since IP effects may last longer in time (on the order of seconds) than inductive effects, the character of the response due to any underlying layer will be obscured, if not completely lost. Only when a deeper layer is so conductive that its vortex current dominates the polarization current will the existence of the deeper layer become apparent (Raiche et al., 1985).

The early-time enhancement in the emf causes the early-

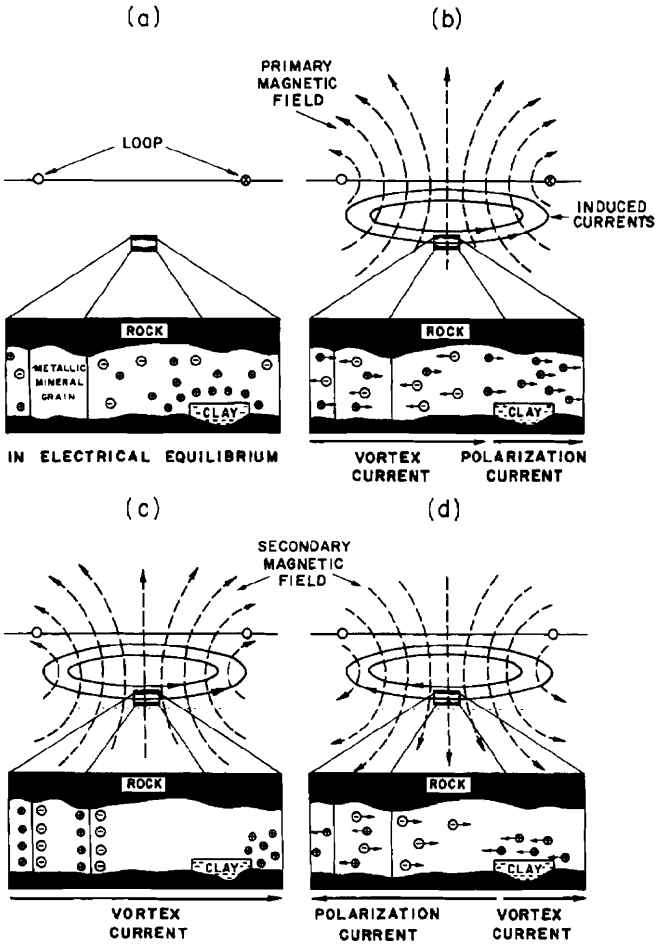

FIG. 3. Schematic diagram of ionic movement in a volume of polarizable rock beneath a TEM transmitter loop. (a) Before transmitter turnoff, ions are in electrical equilibrium with any metallic mineral grains and negatively charged clays present. (b) During turnoff and for a short time thereafter, cations, driven in the same direction as the vortex current, constitute a positive polarization current. (c) At some intermediate time, the ions attain a fully charged state and the polarization current is zero. (d) At later times, the decaying vortex current can no longer support this charged state; the ions drift back to their original positions producing a negative polarization current.

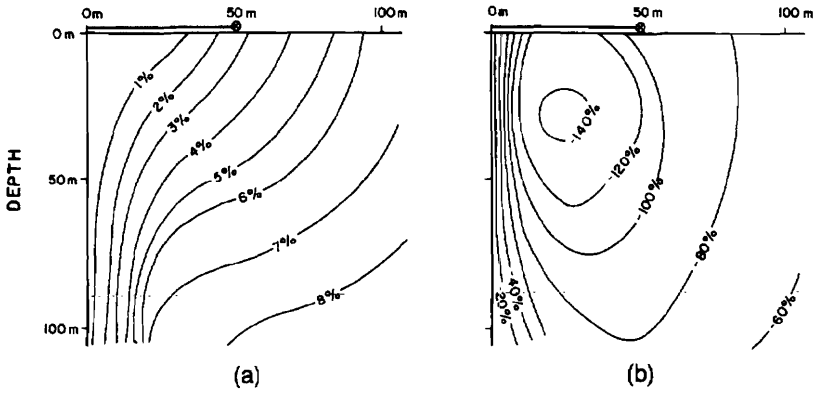

FIG. 4. Contours of the percentage difference between the electric field due to a 500 $\Omega \cdot$ m nonpolarizable half-space and that due to a polarizable half-space with $M = 0.1$, $\tau = 0.001$s, and $c = 0.15$. The transmitter is a 100 m coincident loop centered on 0 m. (a) 0.1 ms after turnoff, (b) 10 ms after turnoff.

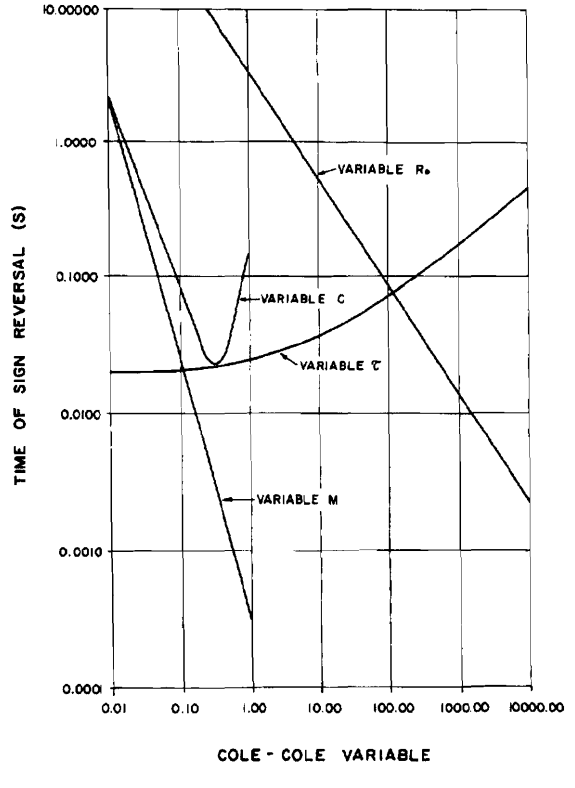

FIG. 5. Time of transient sign reversal against Cole-Cole variable for a half-space. For each curve, three parameters remain fixed, while the fourth is allowed to vary. Fixed values are $R_0 = 500\ \Omega \cdot$ m, $M = 0.1$, $\tau = 1.0$ s, and $c = 0.25$.

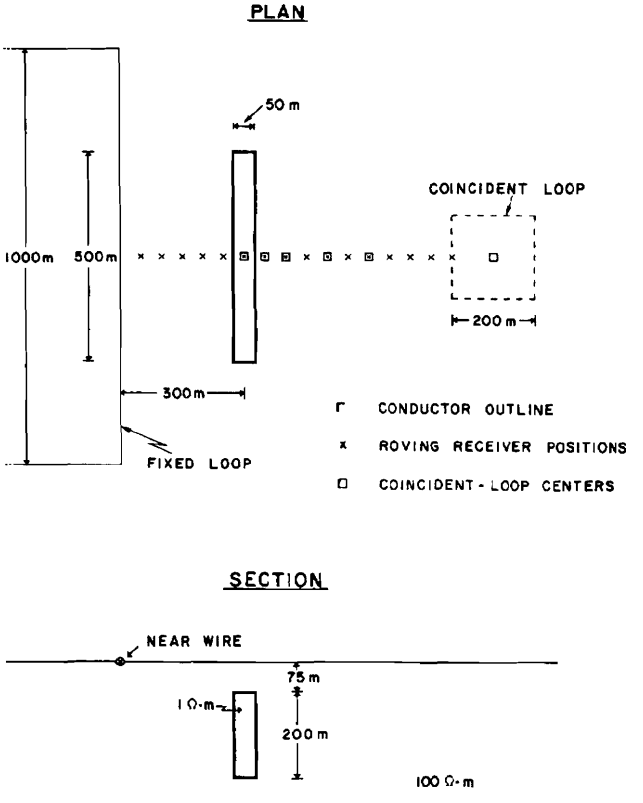

FIG. 6. 3-D conductor studied. Loop configurations consist of a 1000 m x 1000 m fixed loop-roving receiver and a 200 m x 200 m coincident loop.

time resistivities to be underestimated, while the late-time attenuation causes the late-time resistivities to be overestimated. No meaningful resistivities can be derived from a negative transient (Spies and Eggers, 1986). The identification of IP effects in coincident-loop data depends very much on whether a sign reversal or anomalous decay rate is observed. A sign reversal is obvious. Anomalous decay rates may be a little more ambiguous, especially when the earth is not strictly layered. Varying decay rates may cause the interpreter to believe a 3-D structure was present. An increasing decay rate with time may be one criterion for identifying an approaching sign reversal in the transient, but it is not sufficient. Collection of multicomponent data may be required to identify the dimensionality of the earth (Newman and Hohmann, 1987).

THREE-DIMENSIONAL CONDUCTORS

TEM responses due to a 3-D conductor in a half-space were computed using the volume integral equation solution of Newman et al. (1986). Fifty frequencies, ranging from 10^{-3} Hz to 10^{6} Hz, were used to calculate the transient via a discrete convolution approximating a sine transform (Anderson, 1975).

A coincident-loop and a fixed loop-roving receiver configuration were modeled to enable a comparison. Loop sizes were 200 m × 200 m and 1000 m × 1000 m for the coincident-loop and fixed-loop configurations, respectively, the latter having a 1 m^2 receiver. Both loops were energized with a 1 A step-function turnoff with no ramp. The conductor studied is a vertical tabular body with a width of 50 m, strike length of 500 m, depth extent of 200 m, and depth of 75 m (Figure 6). The dc resistivity of the conductor is 1 Ω·m; the half-space resistivity is 100 Ω·m. The choice of models was restricted by the stability of the numerical solution. Deep, low-resistivity contrast conductors were chosen to guarantee precision. Convergence tests, using various conductor discretizations, were undertaken as a check of the solution.

Coincident-loop versus fixed loop-roving receiver

Fixed loop-roving receiver profiles of the vertical component of the time derivative of the magnetic field for the conductor described above are shown in Figure 7. Data for both a nonpolarizable conductor and a polarizable conductor having Cole-Cole parameters $M = 0.95$, $\tau = 10$ s, and $c = 0.25$ are presented. The profiles for the nonpolarizable conductor exhibit relatively simple crossovers and inflections within a half-space response. These crossovers are caused by both induced vortex currents within the conductor and the half-space and galvanic currents induced in the half-space and channeled into the conductor (San Filipo et al., 1985). In the case of the polarizable conductor, a more complex field is evident. At the earliest delay times (not shown), polarization currents start flowing within the conductor in response to the vortex and galvanic currents. By 1 ms, the "smoke ring" in the half-space has diffused past the conductor; the vortex and galvanic currents have decayed significantly; and the polarization current has reversed sign and is dominant. Three crossovers are apparent: that due to the field caused by polarization currents flowing within the conductor (at −12.5 m) and those where the conductor response dominates that of the half-space (at −130 m and 312.5 m). After 3 ms, the polarization current has

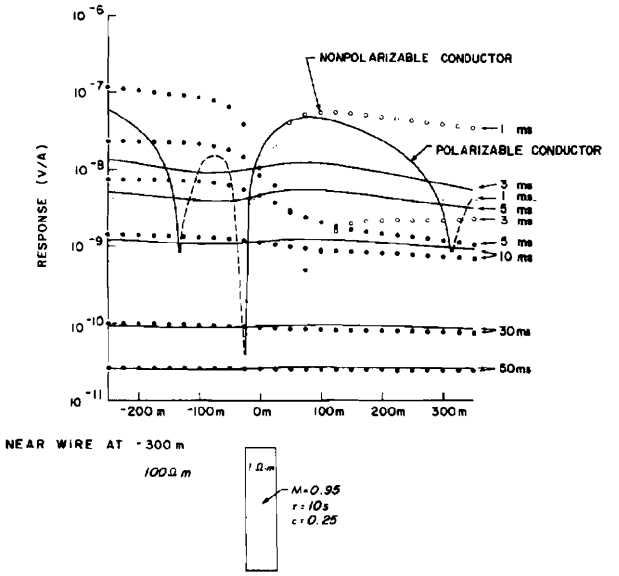

FIG. 7. Profiles for the fixed loop-roving receiver configuration for a polarizable (lines) and nonpolarizable (dots) 3-D conductor in a 100 Ω·m half-space. The geometry of the conductor is shown in Figure 6. Parameters $M = 0.95$, $\tau = 10$ s, and $c = 0.25$ were used for the polarizable case. Solid lines and dots represent positive values; dashed lines and open dots represent negative values.

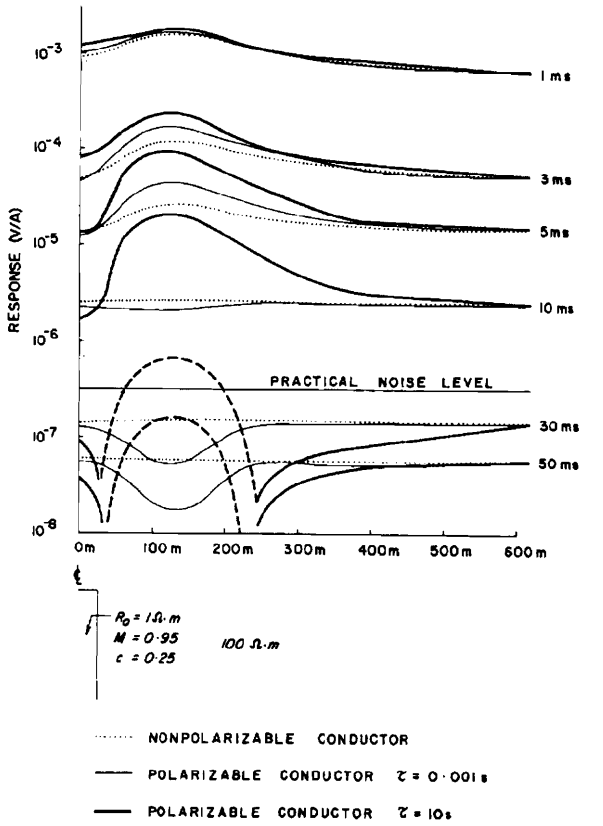

FIG. 8. Coincident-loop profiles for a polarizable (lines) and nonpolarizable (dots) 3-D conductor in a 100 Ω·m half-space. Solid lines and dots represent positive values; dashed lines represent negative values. The geometry of the conductor is shown in Figure 6. Parameters $M = 0.95$, $\tau = 10$ s, and $c = 0.25$ (heavy lines) and $M = 0.95$, $\tau = 0.001$ s, and $c = 0.25$ (light lines) were used for the polarizable cases.

decayed to a level that no longer overwhelmingly dominates the half-space field, resulting in an inflection above the conductor which is in the reverse sense to that expected for a nonpolarizable conductor. This, and the multiple crossovers at early time, may cause confusion to the interpreter.

Coincident-loop profiles for this model are shown in Figure 8. Only half of each profile is shown, since they are symmetric about the conductor. When compared to the nonpolarizable case, the response from the polarizable conductor is enhanced at early delay times and attenuated, or reversed, at late delay times. The mechanisms for this are essentially as described for the layered-earth model. Vortex currents flowing within the conductor are enhanced by the charging polarization currents caused by ionic movement at early delay times, and attenuated by the discharging polarization currents at late delay times. In the 3-D case, however, these currents are not constrained to flow in only the horizontal plane as they are in a 1-D earth. The effects of galvanic currents have not been specifically studied, but such currents may be thought of in the same way as vortex currents: they serve to charge the polarizable conductor. The relative strength, direction, and duration of both the vortex and galvanic current systems ultimately determine in which direction the polarization current flows and whether it is detected.

Effects of host resistivity and depth of burial

With an increase in the host resistivity, events in the transient shift earlier in time (San Filipo and Hohmann, 1985), allowing polarization currents to dominate earlier. Figure 9 shows transients from the 3-D polarizable conductor of Figure 6 imbedded in 100 $\Omega \cdot$m and 200 $\Omega \cdot$m half-spaces. The sign reversal occurs 5 ms earlier for the 200 $\Omega \cdot$m case.

Decreasing the depth of the polarizable conductor also allows the effects of the polarization currents to become obvious earlier. As the current "smoke ring" in the host rock diffuses away from the loop, the field due to the polarization current is able to dominate because it is stationary. Figure 10 compares transients for the polarizable conductor of Figure 6 for three depths: 25, 40, and 75 m. Bringing the conductor from 75 m to 40 m significantly increases the amplitude of the negative part of the decay. Bringing it to 25 m not only further increases the negative amplitude but also shifts the sign reversal at least 5 ms earlier in time.

With even a minor increase in the host rock resistivity, a shallow conductor can produce strong IP effects with moderate Cole-Cole paramcters. Responses for a polarizable conductor at a depth of 40 m in 100 $\Omega \cdot$m and 200 $\Omega \cdot$m half-spaces, and with differing chargeabilities, are shown in Figure

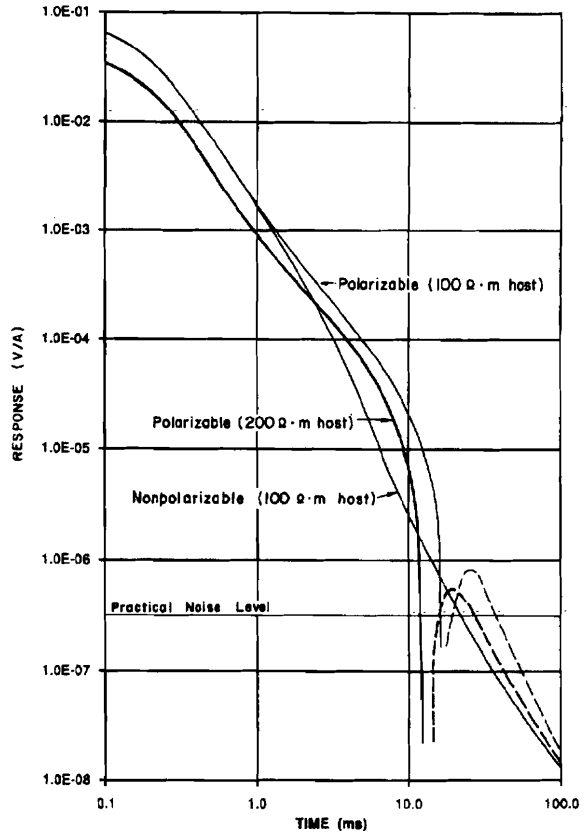

FIG. 9. Coincident-loop transients at station 100 m for a polarizable 3-D conductor ($R_0 = 1\ \Omega \cdot$m, $M = 0.95$, $\tau = 10$ s, $c = 0.25$) in half-spaces of 100 $\Omega \cdot$m and 200 $\Omega \cdot$m. The transient for a nonpolarizable conductor in a 100 $\Omega \cdot$m half-space is also shown. Lines represent positive values; dashes represent negative values.

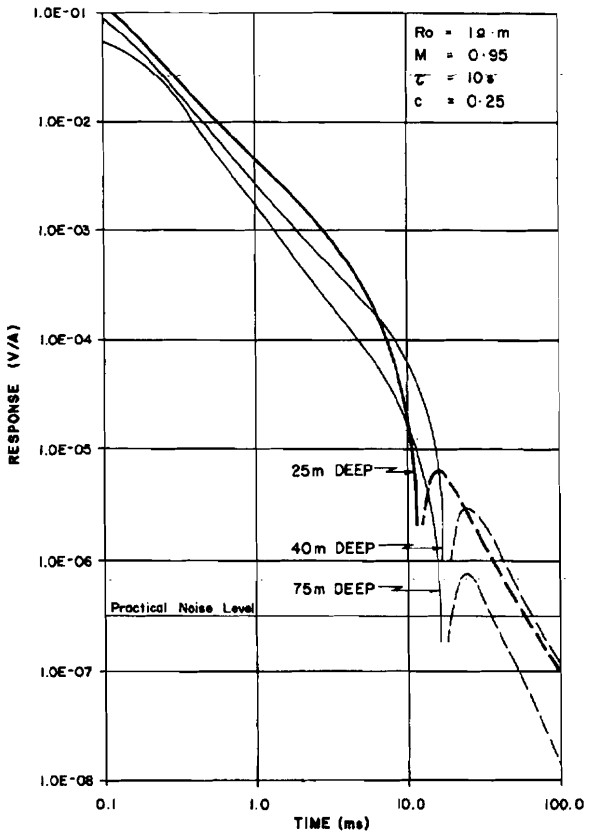

FIG. 10. Coincident-loop transients at station 100 m for a polarizable 3-D conductor ($R_0 = 1\ \Omega \cdot$m, $M = 0.95$, $\tau = 10$ s, $c = 0.25$) at depths of 25, 40, and 75 m in a half-space of 100 $\Omega \cdot$m. Lines represent positive values; dashes represent negative values.

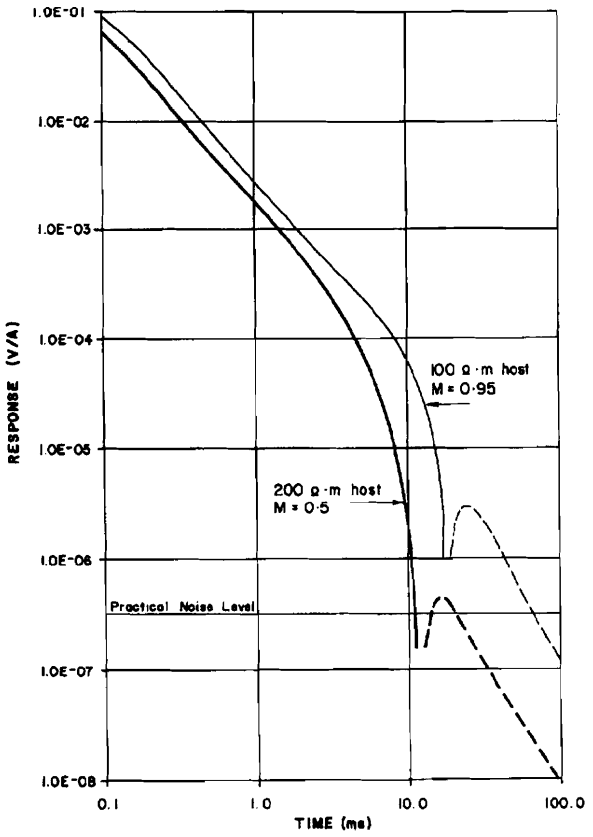

FIG. 11. Coincident-loop transients at station 100 m for a polarizable 3-D conductor at a depth of 40 m. The conductor in a 100 Ω · m half-space has a chargeability of 0.95, while that in a 200 Ω · m half-space has a chargeability of 0.5. Both have $R_0 = 1$ Ω · m, $\tau = 10$ s, and $c = 0.25$. Lines represent positive values, dashes represent negative values.

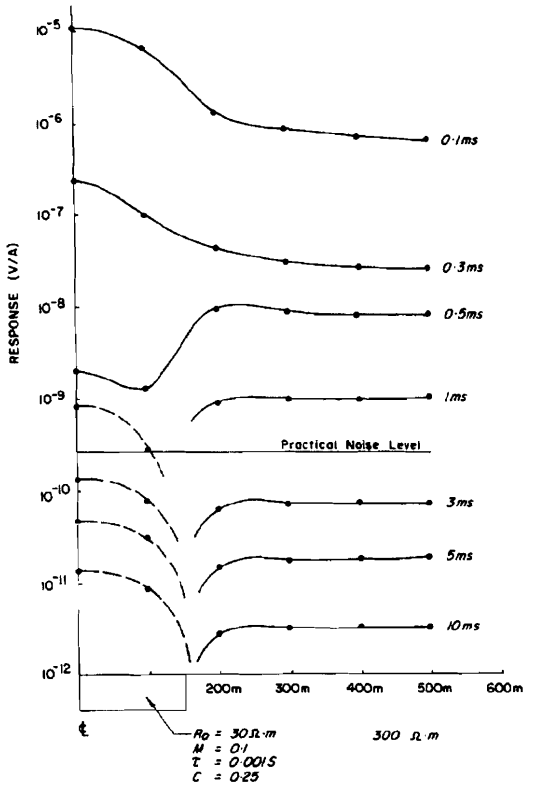

FIG. 13. Response of a surficial polarizable conductor using a 100 m × 100 m in-loop configuration. The model is a flat 300 m × 300 m body, 50 m thick, having a polarizability of $R_0 = 30$ Ω · m, $M = 0.1$, $\tau = 0.001$ s, and $c = 0.25$. The host is non-polarizable with a resistivity of 300 Ω · m. Lines represent positive values; dashes represent negative values; and dots indicate sampling points.

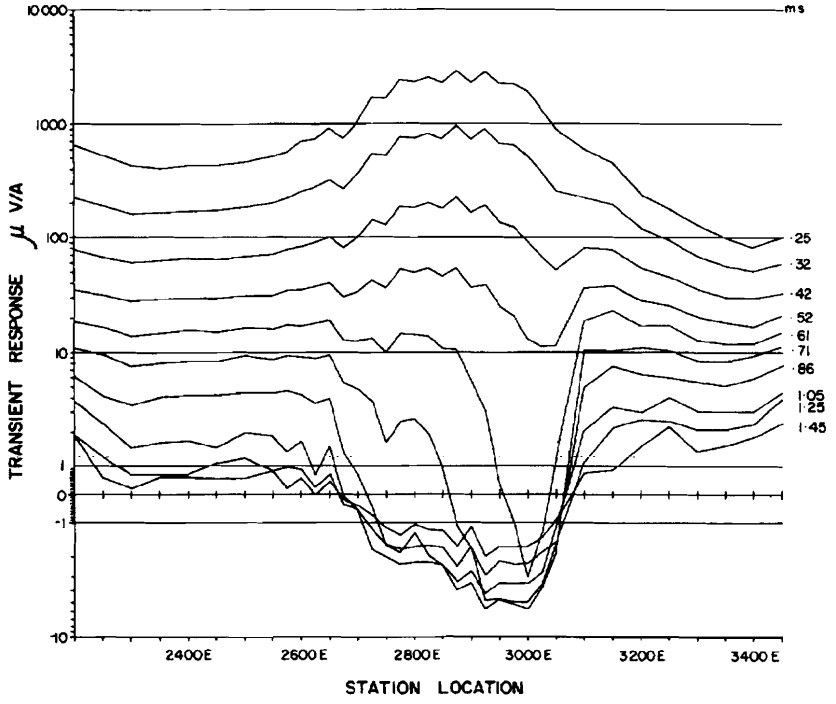

FIG. 12. SIROTEM 100 m × 100 m displaced-loop field data. Loops displaced by 15 m. Numbers on profiles refer to delay times in milliseconds.

11. Even though the conductor in the 200 Ω · m half-space has a chargeability of only 0.5, the IP effects dominate 10 ms earlier than that of the conductor with a chargeability of 0.95 in a half-space of 100 Ω · m.

Interpretation of EM responses

Interpretation of coincident-loop data exhibiting sign reversals has usually been avoided in the past. The transient never attains an invariant TEM time constant, making a choice of constant seemingly impossible. Useful information can still be obtained however. From the results presented here and in the course of this study, it has been established that the spatial characteristics of an anomaly due to a discrete conductor do not change, regardless of the conductor's polarizability. Recognition and interpretation of an anomaly through its diagnostic shape appear to be valid whether the transient reverses or not.

The quality of a conductor is typically interpreted from an EM time constant measured from late delay-time data. Responses at these times are significantly modified by the presence of polarization currents. To obtain an EM time constant which reflects the inductive quality of the conductor, the interpreter is restricted to using only that part of the transient before the drastic increase in decay rate leading to a sign reversal. While this estimated time constant will be in error, the error may not be great enough to warrant concern. In the example of Figure 8, the transient from the station at 600 m was subtracted from that at 100 m to reduce the effects of the host response. Time constants fitted to this transient are 1.2 ms for the nonpolarizable case and 1.7 ms for the polarizable case. This compares well to the true time constant of 1.3 ms (San Filipo et al., 1985). In all cases studied, the EM time constant was within a factor of two of the true value. Quantitative information regarding the IP parameters of the conductor cannot be obtained from the negative part of the transient, since this decay is due to at least two exponentials: that due to the decay of the vortex currents and that due to the decay of the polarization current (Snyder, 1980). Qualitative information, such as slow decays indicating large IP time constants, may be obtained; but further investigation is required.

FIELD EXAMPLE

Figure 12 shows coincident-loop data collected with an early-time SIROTEM system (Buselli, 1985). The loop, deployed in the displaced mode to overcome superparamagnetic effects, was 100 m × 100 m. The geology in the area consists of steeply dipping pelites, psammites, and psammo-pelites. Shearing is common, and surficial sands and clays are ubiquitous.

A broad anomaly located between 2650E and 3100E reverses sign at 0.61 ms, indicating a polarizable conductor is

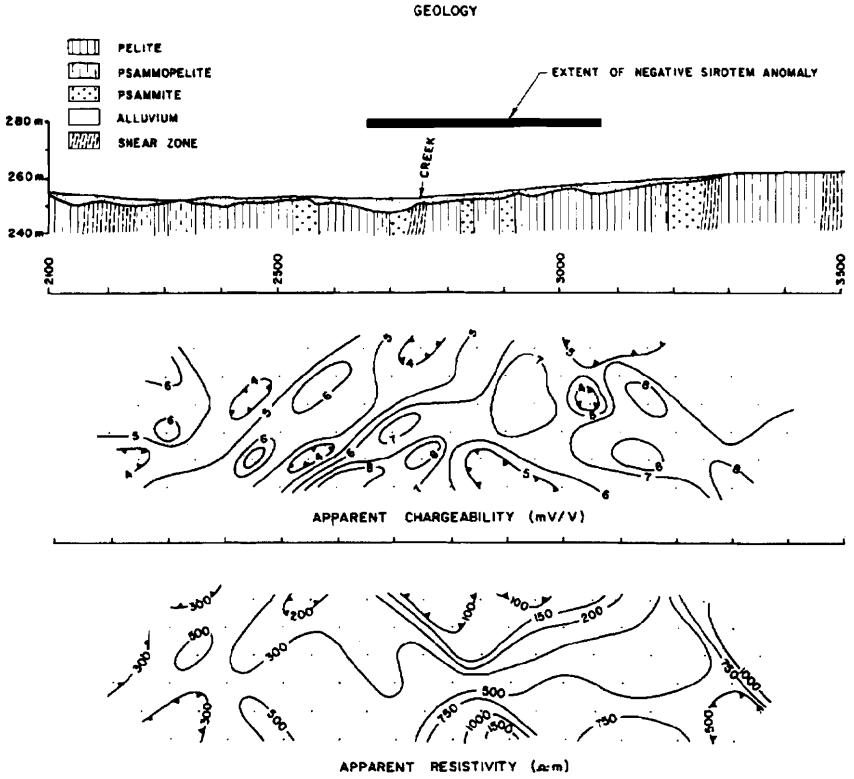

FIG. 14. Time-domain IP section and summary geology for the profile shown in Figure 12. Dipole-dipole length is 100 m.

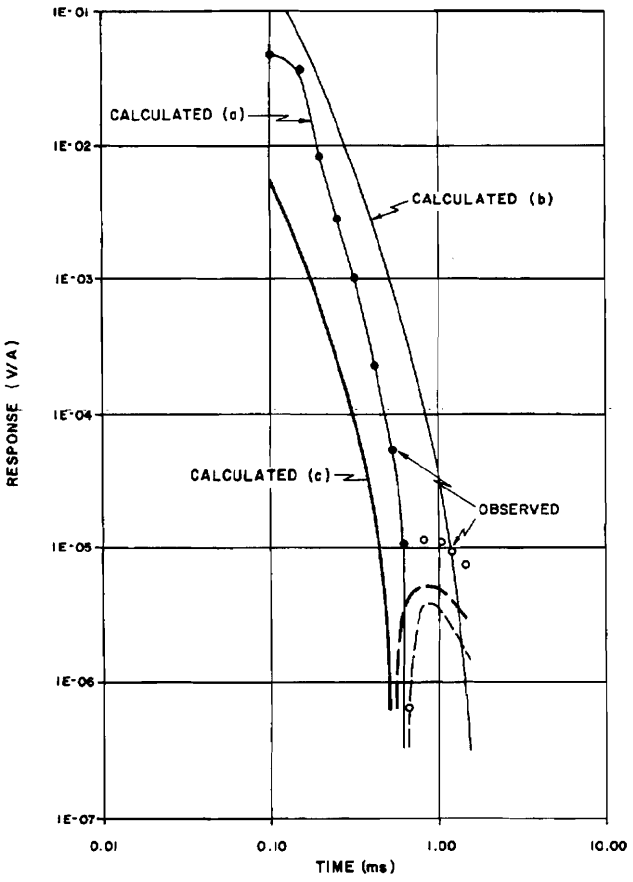

FIG. 15. Observed (circles) and calculated (lines) transients for station 2875E of the profile shown in Figure 12. Polarizabilities for the surficial layer are: calculated(a) $R_0 = 22\ \Omega\cdot$m, $M = 0.13$, $\tau = 0.01$ s, and $c = 0.25$; calculated(b) $R_0 = 8.6\ \Omega\cdot$m, $M = 0.123$, $\tau = 3.1$E–4 s, and $c = 0.25$; and calculated(c) $R_0 = 56\ \Omega\cdot$m, $M = 0.209$, $\tau = 0.0145$ s, and $c = 0.25$. In all cases, basement has $R_0 = 600\ \Omega\cdot$m, $M = 0.05$, $\tau = 0.01$ s, and $c = 0.25$. Lines and dots represent positive values; dashes and open circles represent negative values.

present. The anomaly's shape is quite definitive before the sign reversal. In particular, shoulders at 2650E and 3100E are suggestive of a surficial conductor. Numerical modeling of a discrete surficial polarizable conductor using an in-loop configuration results in a similar set of profiles (Figure 13). Although sampling density is not high enough to define the edge effects expected from such a conductor, this model nonetheless illustrates the ease with which such anomalies may be generated.

A time-domain 100 m dipole-dipole IP survey carried out over the TEM anomaly mapped a surficial resistivity low between 2500E and 3100E, confirming the interpretation (Figure 14). Note that no particularly strong apparent chargeability anomaly is present. Forward modeling of the TEM transient at station 2875E gives a 15 m thick surficial layer with $R_0 = 22\ \Omega\cdot$m, $M = 0.13$, $\tau = 0.01$s, and $c = 0.25$ overlying a basement with $R_0 = 600\ \Omega\cdot$m, $M = 0.05$, $\tau = 0.01$s, and $c = 0.25$, the extent of the anomaly being sufficient to apply a 1-D model. The observed and calculated TEM transients are compared in Figure 15. Inverting the $n = 1$ IP data from station 2850E to the Cole-Cole model (Anderson and Smith, 1984) gives $R_0 = 56\ \Omega\cdot$m ($\pm$0.01), $M = 0.209$ ($\pm$0.05), $\tau = 1.4$E–2 s ($\pm$3.0E-4), and $c = 0.25$ (fixed) for the 100 m dipole-dipole survey and $R_0 = 8.6\ \Omega\cdot$m ($\pm$0.01), $M = 0.091$ ($\pm$0.032), $\tau = 2.8$E–4 s ($\pm$3.0E-5), and $c = 0.25$ (fixed) for a 2 m dipole-dipole spot measurement from the same location. Applying these sets of parameters to the surficial layer to generate TEM transients results in the curves shown in Figure 15. In both cases, the weakly polarizable basement had to be included to obtain an agreeable decay, although the basement by itself generates no sign reversal. The observed transient lies between those predicted by the 2 m and 100 m dipole IP data, but in neither case was the amplitude of the observed negative matched. A confined surficial polarizable conductor may give more comparable results. The vortex currents induced in a confined conductor will be of a lower amplitude than those induced in a layer having the same Cole-Cole parameters, allowing the polarization current to dominate earlier and with a higher amplitude.

CONCLUSIONS

Sign reversals in coincident-loop TEM data can be explained by IP effects. These effects may be considered in terms of the classic IP model but with the substitution of an induced vortex current for the usual directly injected current. A polarization current, caused by the movement of ions in the polarizable rock and driven by the vortex current, reverses sign as it changes from a charging to a discharging current.

In a layered earth, a sign reversal in the transient occurs when the polarization current dominates the vortex current. The time of the sign reversal is most dependent on the dc resistivities and polarizabilities of the layers; these control the strength of the vortex and polarization currents, respectively. In the case of a 3-D conductor in a conductive host, the presence of a host response serves to delay the time at which polarization currents dominate. Increasing the resistivity of the host allows the polarization current to dominate earlier by reducing the host response. Additionally, reducing the depth of the conductor causes the signal to be of sufficiently large amplitude and early enough in time to be measurable. Confined, weakly polarizable conductors may produce strong IP effects if they are at or very near the surface. Deep conductors need to be strongly polarizable and occur in a resistive host to exhibit similar effects.

With careful application of the normal interpretation procedures, conductor quality and geometry can be assesed in the presence of IP effects. While further studies are required to determine the interpretability of other conductor characteristics, such as dip and depth, indications are that such interpretations would be valid.

ACKNOWLEDGMENTS

We are indebted to Walt Anderson and the late Frank Frischknecht for putting the USGS Vax-11/780 computer at our disposal. For his continual support, we wish to thank Bob Smith of CRA Exploration Pty. Ltd. The funding for this work was provided by CRA Exploration Pty. Ltd.

REFERENCES

Anderson, W. L., 1975, Improved digital filters for evaluating Fourier and Hankel transformation integrals: Nat. Tech. Inf. Serv. rep. PB 242-800.

Anderson, W. L., and Smith, B. D., 1984, Nonlinear least-squares inversion of transient induced polarization data (program NLSTIP):U.S. Geol. Surv. Rep. 84-515.

Buselli, G., 1985, Stratigraphic mapping applications of TEM: Explor. Geophys., **16**, 177–179.

Dyck, A. V., Bloore, M., and Vallee, M. A., 1980, EM response of a rectangular thin plate conductor, user manual: Research in Applied Geophysics (Univ. of Toronto), no. 14.

Hohmann, G. W., Kintzinger, P. R., Van Voorhis, G. D., and Ward, S. H., 1970, Evaluation of the measurement of induced electrical polarization with an inductive system: Geophysics, **35**, 901–915.

Knight, J. H., and Raiche, A. P., 1982, Transient electromagnetic calculations using the Gaver-Stehfest inverse Laplace transform method: Geophysics, **47**, 47–50.

Lee, T. J., 1975, Sign reversals in the transient method of electrical prospecting (one-loop version): Geophys. Prosp., **23**, 453–462.

——— 1981, Transient electromagnetic response of a polarizable ground: Geophysics, **46**, 1037–1041.

Lewis, J. G., and Lee, T. J., 1984, The detection of induced polarization with a transient electromagnetic system: Inst. Elect. Electron. Eng., Trans. Geosci. Remote Sensing, **GE-22**, 69–80.

Lewis, J. G., and Bishop, J. R., 1988, Inversion of time domain spectral IP data: Explor. Geophys., **19**, 303–305.

Morrison, H. F., Phillips, R. J., and O'Brien, D. P., 1969, Quantitative interpretation of transient electromagnetic fields over a layered halfspace: Geophys. Prosp., **17**, 82–101.

Newman, G. A., Hohmann, G. W., and Anderson, W. L., 1986, Transient electromagnetic response of a three-dimensional body in a layered earth: Geophysics, **51**, 1608–1627.

Newman, G. A., and Hohmann, G. W., 1987, Interpretation of TEM soundings over 3-D structures with the central-loop configuration: Geophys. J. Roy. Astr. Soc., **89**, 889–914.

Ogilvy, R. D., 1983, A model study of the transient electromagnetic coincident loop technique: Geoexplor., **21**, 231–264.

Pelton, W. H., 1977, Interpretation of induced polarization and resistivity data: Ph.D. dissertation, Univ. of Utah.

Raiche, A. P., 1983, Negative transient voltage and magnetic field responses for a half-space with Cole-Cole impedance: Geophysics, **48**, 790–791.

Raiche, A. P., Bennett, L. A., Clark, P. J., and Smith, R. J., 1985, The use of Cole-Cole impedances to interpret the TEM response of layered earths: Expl. Geophys., **16**, 271–272.

San Filipo, W. A., and Hohmann, G. W., 1985, Intergal equation solution for the transient electromagnetic response of a three-dimensional body in a conductive half-space: Geophysics, **50**, 798–809.

San Filipo, W. A., Eaton, P. A., and Hohmann, G. W., 1985, The effect of a conductive half-space on the transient electromagnetic response of a three-dimensional body: Geophysics, **50**, 1144–1162.

Sidorov, V. A., and Yakhin, A. M., 1979, Induced polarization in rocks with inductive excitation: Izv. Acad. Sci. U.S.S.R. Phys. Solid Earth, **15**, 810–814.

Snyder, D. D., 1980, *in* Sumner, J. S., and Zonge, K. L., Eds., Induced polarization for exploration geophysicists: South African Geophys. Assoc.

Spies, B. R., 1980a, A field occurrence of sign reversals with the transient EM method: Geophys. Prosp., **28**, 620–632.

——— 1980b. Results of experimental and test TEM surveys, Elura deposit, Cobar, NSW: Bull., Austral. Soc. Expl. Geophys., **11**, 289–294.

Spies, B. R., and Eggers, D. E., 1986, The use and misuse of apparent resistivity in electromagnetic methods: Geophysics, **51**, 1462–1479.

Sumner, J. S., 1976, Principles of induced polarization for geophysical exploration: Elsevier Science Publ. Co., Inc.

Wait, J. R., and Debroux, P., 1984, Induced polarization in electromagnetic inductive schemes: Geophys. Prosp., **32**, 1147–1154.

Weidelt, P., 1982, Response characteristics of coincident-loop transient electromagnetic systems: Geophysics, **47**, 1325–1330.